

Izvestiya Vysshikh Uchebnykh Zavedeniy. Applied Nonlinear Dynamics. 2023;31(5)

Article

DOI: 10.18500/0869-6632-003067

Study of character of modulation instability in cyclotron resonance interaction of an electromagnetic wave with a counterpropagating rectilinear electron beam

A. A. Rostuntsova^{1,2,3}✉, N. M. Ryskin^{1,3}

¹Saratov Branch of Kotelnikov Institute of Radioengineering and Electronics of the RAS, Russia

²A. V. Gaponov-Grekhov Institute of Applied Physics of the RAS, Nizhny Novgorod, Russia

³Saratov State University, Russia

E-mail: ✉rostuncova@mail.ru, ryskinm@info.sgu.ru

Received 14.07.2023, accepted 4.09.2023, available online 19.09.2023, published 29.09.2023

Abstract. In this paper, the interaction of a monochromatic electromagnetic wave with a counterpropagating electron beam moving in an axial magnetic field is considered. The *purpose* of this study is to investigate the conditions for occurrence of modulation instability (MI) in such a system and to determine at which parameters of the incident wave the MI is absolute or convective. *Methods.* Theoretical analysis of the MI character is carried out by studying the asymptotic form of unstable perturbations using the saddle-point analysis. The analytical results are verified by numerical simulations. *Results.* Theoretically, the boundary of change in the character of MI on the plane of input signal parameters (amplitude and detuning of the frequency from the cyclotron resonance) is determined. Numerical simulations confirm that as the signal frequency increases, the regime of self-modulation, which corresponds to the absolute MI, is replaced by the stationary single-frequency transmission corresponding to the convective MI. The numerical results coincide with the analytical ones for the system, which is matched at the end. The matching is implemented by smooth increasing of the guiding magnetic field in the region of electron beam injection. *Conclusion.* Determining the analytical conditions for the implementation of the absolute MI is of practical interest, since the emerging self-modulation can lead to the generation of trains of pulses with the spectrum in the form of frequency combs.

Keywords: modulation instability, absolute/convective instability, nonlinear waves, microwave solitons, cyclotron resonance.

Acknowledgements. This work was supported by Russian Science Foundation under Grant No. 23-12-00291.

For citation: Rostuntsova AA, Ryskin NM. Study of character of modulation instability in cyclotron resonance interaction of an electromagnetic wave with a counterpropagating rectilinear electron beam. *Izvestiya VUZ. Applied Nonlinear Dynamics.* 2023;31(5):597–609. DOI: 10.18500/0869-6632-003067

This is an open access article distributed under the terms of Creative Commons Attribution License (CC-BY 4.0).

Introduction

One of the fundamental effects leading to the emergence of complex dynamics in nonlinear media with dispersion is the modulation instability (MI) [1–6]. MI is the instability of a monochromatic wave with a carrier frequency ω with respect to slow spatio-temporal modulations at the side frequencies $\omega \pm \Omega$, $\Omega \ll \omega$. MI can be observed in systems of various nature and plays an important role in nonlinear optics, plasma physics, hydrodynamics, etc.

In the presence of MI, the harmonic signal propagating in a nonlinear medium with dispersion is enriched with new independent spectral components. Instead of stationary wave propagation, self-modulation is observed, that is, wave amplitude oscillations, which can be both regular and chaotic. The process of MI development, as a rule, ends with the formation of envelope solitons. The most famous example of such solitons are the soliton solutions of the nonlinear Schrödinger (NLS) equation [2–6].

In a medium with a finite length excited by a harmonic signal at one of the boundaries, the wave propagation process significantly depends on whether the MI is convective or absolute [6,7]. In the works [8,9], the differences between convective and absolute MI were investigated using the example of relatively simple model systems described by the NLS equation or the nonlinear Klein–Gordon equation. In convective instability, unstable perturbations move along the system and leave it. Thus, after the transient process, the regime of stationary wave propagation is established. Nonstationary regimes of self-modulation are observed only in the case of absolute MI, when unstable perturbations are continuously generated along the entire length of the system.

In the work [10], we investigated MI in the cyclotron resonance interaction of an electromagnetic wave (EMW) with a counterpropagating, initially rectilinear beam of electrons moving in an axial magnetic field. The beam acts as a nonlinear medium consisting of non-isochronous electron-oscillators. The nonisochronicity is due to the relativistic dependence of the cyclotron frequency on the electron energy. When the frequency of the incident monochromatic EMW is within the cyclotron absorption band, and the signal power is sufficiently small, the wave attenuates and at the same time the transverse oscillations of the electrons are excited. However, with an increase in the signal amplitude, the absorption band shifts to the region of lower frequencies due to the non-isochronous oscillations of the electrons. As a result, EMW propagation without attenuation becomes possible. At the same time, due to the development of MI, the input signal can be transformed into a train of microwave solitons. Note that a similar effect was first predicted in [11], where it was called nonlinear or soliton tunneling (see also [3]). With respect to the system considered in this paper, it was discovered and investigated in the works [12–14]. The implementation of this effect in microwave electronics is of obvious interest from the point of view of generating trains of short microwave pulses with a spectrum in the form of frequency combs, which is relevant for a number of practical applications, for example, in spectroscopy [15,16].

Theoretical analysis of nonlinear stationary solutions in the form of solitons allowed us to determine an analytical condition for the amplitude and frequency of the incident EMW, in which cyclotron absorption is replaced by self-modulation, and the found condition agrees well with the results of numerical simulation [10]. In addition, it was found that with an increase in the frequency of the input signal, the nonstationary regime of self-modulation is replaced by the stationary propagation of the wave. In this paper, it is shown that this effect is associated with a change in the nature of MI from absolute to convective. The results of theoretical analysis of the nature of MI are presented, in particular, a rigorous study of the asymptotic form of unstable perturbations by the saddle-point analysis is carried out. As a result, the analytical boundary of the transition from absolute MI to convective on the plane of the input signal parameters is determined. The theoretical conclusions are confirmed by the results of numerical simulation.

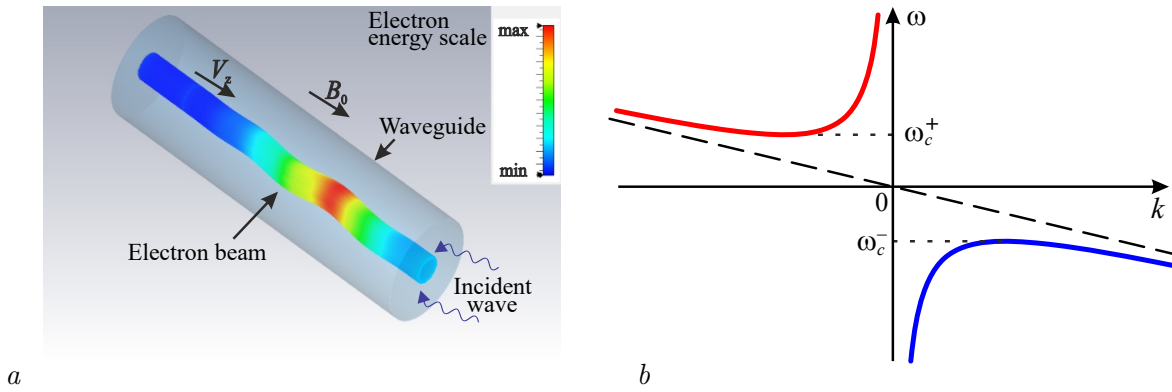


Fig 1. *a* – scheme of the resonance cyclotron interaction of radiation with a counterpropagating rectilinear electron beam; *b* – dispersion diagram $\omega(k)$ (color online)

1. Model and basic equations

The scheme of the considered model is shown in Fig. 1, *a*. A annular electron beam guided by a uniform axial magnetic field B_0 interacts with a backward wave in a cylindrical waveguide under the cyclotron resonance condition

$$\omega_r + h_r V_z \approx \omega_H, \tag{1}$$

where ω_r and $h_r = h_r(\omega_r)$ are frequency and propagation constant of the wave, respectively, V_z is longitudinal velocity of electrons, $\omega_H = eB_0/(m_e\gamma)$ is the cyclotron frequency, e and m are the charge and rest mass of the electron, γ is the Lorentz factor. Electrons rotating in an axial magnetic field are cyclotron oscillators that are non-isochronous due to the relativistic dependence of the cyclotron rotation frequency on energy $\omega_H = \omega_H(\gamma)$. It is assumed that the electrons have no transverse velocity at the entrance to the interaction space. Such a beam forms a passive medium of non-isochronous cyclotron electron-oscillators, unlike cyclotron resonance masers, where a beam of rotating electrons, which is an active medium, enters the electromagnetic structure. The EMW propagating towards the beam of unexcited electron-oscillators, when the condition (1) is met, begins to be absorbed, causing transverse oscillations of the electrons. With an increase in the amplitude of these oscillations, the cyclotron resonance condition (1) is violated, and the absorption is saturated.

The electron-wave interaction in the model under consideration is described by the system of equations well known from the literature [10, 12–14]:

$$\frac{\partial a}{\partial \tau} - \frac{\partial a}{\partial Z} = -p, \tag{2}$$

$$\frac{\partial p}{\partial Z} + i|p|^2 p = a. \tag{3}$$

Here (2) is the equation of wave excitation by an electron beam, and (3) is the equation of electron motion in the wave field averaged over the period of cyclotron oscillations. In the equations (2), (3) a is the normalized slowly varying complex amplitude of the wave field, $p = p_x + ip_y$ is the normalized transverse momentum of electrons, $Z \sim z$ and $\tau \sim (t - z/V_z)$ are dimensionless independent variables, x, y are transverse coordinates, z is longitudinal coordinate, and t is time. All variables in (2) are dimensionless, for more information, see [10, 12–14]. Since the electron beam at $Z = 0$ has zero rotational velocity, the boundary condition is

$$p(Z = 0) = 0. \tag{4}$$

At the right boundary of the system, at $Z = L$, where L is a dimensionless length, an external harmonic signal is applied, that is

$$a(Z = L) = A_0 e^{i\omega\tau}, \quad (5)$$

where A_0 and ω are the normalized amplitude and frequency detuning of the signal from the frequency of cyclotron resonance, respectively.

2. Nonlinear dispersion relation

Consider the solutions of the equations (2), (3) in the form of a monochromatic wave with constant amplitude: $a = A_0 e^{i(\omega\tau - kZ)}$, $p = P_0 e^{i(\omega\tau - kZ)}$. In [10], the nonlinear dispersion relation was obtained for these solutions

$$(\omega + k) (k - |P_0|^2) = -1, \quad (6)$$

moreover, the complex amplitudes of the waves A_0 and P_0 satisfy the relation

$$|P_0|^2 = |A_0|^2 (\omega + k)^2. \quad (7)$$

Analysis of the equation (6) shows that there is a non-transmission band $\omega_c^- < \omega < \omega_c^+$, whose boundaries $\omega_c^\pm = \pm 2 - |A_0|^2$ are shifted to the region of lower frequencies with an increase in the amplitude of the wave. A qualitative view of the dispersion diagram is shown in Fig. 1, b. For waves with $\omega > \omega_c^+$ corresponding to the upper branch of the dispersion characteristic, the Lighthill criterion is met [2-6]

$$\chi\beta > 0, \quad (8)$$

testifying to the presence of MI. Here $\chi = \partial^2\omega/\partial k^2$ is the group velocity dispersion parameter, and $\beta = -\partial\omega/\partial|A_0|^2$ is the parameter of nonlinearity. Taking into account (6), it is not difficult to find expressions for these parameters:

$$\chi = -\frac{2}{(k - |P_0|^2)^3}, \quad \beta = \frac{1}{(k - |P_0|^2)^4}. \quad (9)$$

If one selects the frequency of the input harmonic signal in the non-transmission band and starts increasing its amplitude, sooner or later this frequency will be equal to the critical ω_c^+ . Instead of cyclotron absorption, propagation of undamped waves (nonlinear tunneling) will become possible. However, the analysis of the nonlinear dispersion relation is carried out for an infinite medium, whereas the system under consideration is fundamentally limited in space, since the boundary conditions (4), (5) are placed at different ends of the interaction space. As shown in [10], the critical value of the frequency at which EMW propagation begins differs from ω_c^+ and is determined by the equation

$$\omega = 2 - \frac{1}{2}|A_0|^2. \quad (10)$$

Note that (10) exactly corresponds to the relation between the frequency and amplitude of the exact solution in the form of a soliton [10, 12-14]. Indeed, MI causes the tunneling wave to split into traveling envelope solitons (see [10]).

3. Analysis of the nature of modulation instability

To determine the nature of instability (absolute or convective), we will investigate the asymptotic form of unstable perturbations at infinitely large times [7, 18, 19]. Since MI is the instability of a monochromatic wave with respect to slow modulations with frequencies lying in a small interval near the carrier frequency, we will define small perturbations of the monochromatic solution

$$\begin{aligned} a &= (A_0 + \tilde{a}(Z, \tau)) e^{i(\omega\tau - kZ)}, \\ p &= (P_0 + \tilde{p}(Z, \tau)) e^{i(\omega\tau - kZ)}, \end{aligned} \quad (11)$$

where $|\tilde{a}(Z, \tau)| \ll |A_0|$, $|\tilde{p}(Z, \tau)| \ll |P_0|$, and ω and k satisfy the dispersion relation (6). Following [6–9], we will look for a solution in the form of a pair of satellites equidistant from the carrier frequency:

$$\begin{aligned} \tilde{a} &= a_+ e^{i(\Omega\tau - KZ)} + a_- e^{-i(\Omega\tau - KZ)}, \\ \tilde{p} &= p_+ e^{i(\Omega\tau - KZ)} + p_- e^{-i(\Omega\tau - KZ)}. \end{aligned} \quad (12)$$

After substituting (11) and (12) into the original equations (2), (3) and linearization of the system, we obtain the dispersion relation for the frequency Ω and the wave number K of small perturbation. The roots of this equation can be written explicitly:

$$\Omega(K) = -K + \frac{K(\omega + k)^2}{1 + (\omega + k)^2(K_0^2 - K^2)} \pm \frac{K(\omega + k)^2 \sqrt{(\omega + k)^2(K^2 - K_0^2)}}{1 + (\omega + k)^2(K_0^2 - K^2)}, \quad (13)$$

where the notation $K_0^2 = 2|P_0|^2/(\omega + k)$ is introduced. Recall that we consider the upper branch of the dispersion characteristic, where MI occurs (see Fig. 1, b). In this case, $(\omega + k) > 0$ and $K_0^2 > 0$.

If we consider K to be real, in the domain of wave numbers $K^2 < K_0^2$ the roots $\Omega(K)$ will be complex. For the instability increment $\lambda = -\text{Im}[\Omega(K)]$ we get the following expression:

$$\lambda(K) = |K| \frac{(\omega + k)^3 \sqrt{K_0^2 - K^2}}{1 + (\omega + k)^2(K_0^2 - K^2)}. \quad (14)$$

It follows from (14) that MI actually occurs on the upper branch of the dispersion characteristic, which corresponds to the conclusions based on the Lighthill criterion (see section 2). Figure 2 shows the dependence of the instability increment on K and $|P_0|$. It can be seen that with an increase in the amplitude of the wave, the region of wave numbers in which MI occurs expands.

For a more rigorous analysis, we will consider both Ω and K complex. Following [7, 18, 19], we present a general solution for a small field perturbation in the form of a Fourier integral

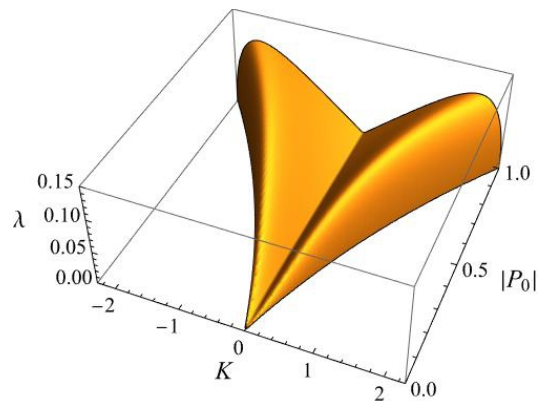


Fig 2. Increment of the MI $\lambda(K)$ as a function of K and $|P_0|$ at $\omega = 2$

$$\tilde{a}(Z, \tau) = \int_{-\infty}^{+\infty} a_K e^{i(\Omega(K)\tau - KZ)} dK. \quad (15)$$

The asymptotic form of the integral (15) under the condition $\tau \rightarrow \infty$ is estimated by the saddle-point analysis. In doing so,

$$\tilde{a}(Z, \tau) \sim \frac{1}{\sqrt{\tau}} e^{-\text{Im}[\Omega(K_s)]\tau}, \quad (16)$$

where K_s is the saddle point where $d\Omega(K_s)/dK - Z/\tau = 0$ [7, 18, 19].

Instability is absolute if at any fixed point Z at $\tau \rightarrow \infty$ the perturbation increases infinitely in time. According to the estimate (16), this condition corresponds to the inequality

$$\text{Im}[\Omega(K_s)] < 0. \quad (17)$$

The saddle point in the limit $Z/\tau \rightarrow 0$ is determined from the condition of zero complex group velocity

$$\frac{d\Omega}{dK} = 0. \quad (18)$$

In this case, the integration contour in (15) is deformed in such a way as to pass through the saddle point along the line of the steepest descent.

The equation (18) is solved numerically together with the dispersion relation (13). There are a total of 6 saddle points K_s^i , which correspond to the roots $\Omega_i(K_s)$, $i = 1, \dots, 6$. We number them as shown in Fig. 3, where an example of the dependencies of $\text{Re}\Omega_i$ and $\text{Im}\Omega_i$ on the carrier

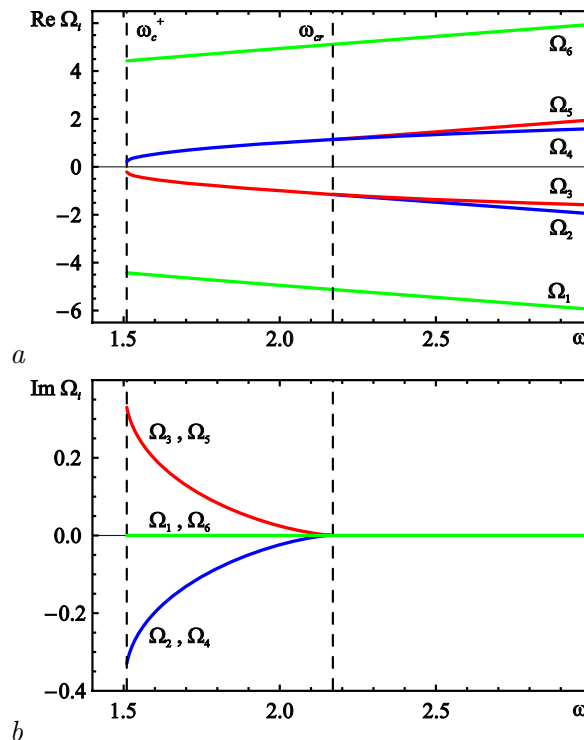


Fig 3. Dependences of the real (a) and imaginary (b) parts of the roots of the characteristic equation Ω_i on the carrier frequency ω at $|P_0| = 0.7$. The critical value $\omega_{cr} = 2.18$ corresponds to the change of the character of MI (color online)

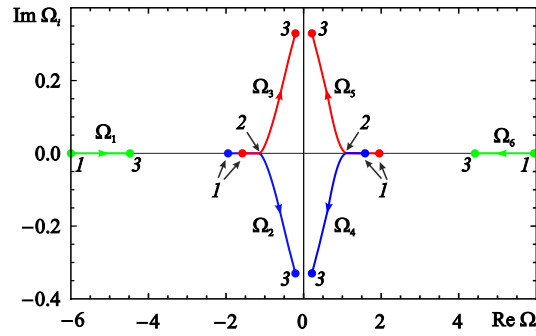


Fig 4. Positions of the roots Ω_i in the complex plane as the frequency decreases from $\omega = 3.00$ (points 1) to the cutoff frequency $\omega_c^+ = 1.51$ (points 3) at $|P_0| = 0.7$. The critical value $\omega_{cr} = 2.18$ (points 2) corresponds to the change of the character of MI (color online)

frequency ω at some fixed value $|P_0|$ is given. The roots have symmetry $\Omega_{1,2,3} = -\Omega_{6,5,4}$, which is obviously due to the choice of a perturbation in the form of a pair of symmetric satellites (see (12)).

For any fixed amplitude $|P_0|$, there is some critical value of the carrier frequency $\omega = \omega_{cr}$, such that for $\omega > \omega_{cr}$ all saddle points K_s lie on the real axis. The corresponding roots of the dispersion relation (13) are also real, that is, $\text{Im}[\Omega(K_s)] = 0$. This means that at $\omega > \omega_{cr}$ the condition (17) is not met, therefore, MI is convective.

When the frequency ω becomes below the critical value, two pairs of saddle points with a nonzero imaginary part appear in the K -plane. The corresponding roots Ω_i become complex conjugate: $\Omega_2 = \Omega_3^*$, $\Omega_4 = \Omega_5^*$ (see Fig. 3). The roots Ω_1, Ω_6 remain real numbers. Obviously, in each pair of complex-conjugate roots, the condition (17) is fulfilled for one of them, therefore MI is absolute.

Fig. 4 illustrates the change in the position of the roots in the complex plane when changing ω . With a decrease in ω , the real parts of complex roots decrease in absolute value, and the imaginary ones, on the contrary, increase. When the carrier frequency becomes less than the cutoff frequency ω_c^+ , the wave becomes attenuated and it obviously makes no sense to talk about MI.

4. Numerical simulation

Compare the results of theoretical analysis of the nature of MI with numerical simulation. The equations (2), (3) with boundary conditions (4), (5) were integrated using an explicit finite-difference scheme of the second-order accuracy for both independent variables.

In Fig. 5 the partitioning of the parameter plane $(\omega, |A_0|)$ on the areas of various dynamic regimes is presented. The dashed line shows the boundary of the non-transmission band, below which, in region 1, the input signal attenuates. This boundary is completely consistent with the theoretical formula (10). Above it, in region 2, the wave propagation is non-stationary, that is, self-modulation regimes are observed. In this area, MI is absolute. Note that near the boundary, close-to-periodic trains of traveling solitons are generated, however, as we move away from the boundary, the shape of the generated signal begins to have a complex, irregular character (for more information, see [10]).

In region 3, where the MI becomes convective, after a certain transient process, the regime of stationary wave propagation is established. The established dependencies $|a(Z)|$ and $|p(Z)|$ are periodic. The corresponding analytical solutions were found in [10]. The solid line in Fig. 5 corresponds to the analytical boundary of the change in the character of MI. For its construction,

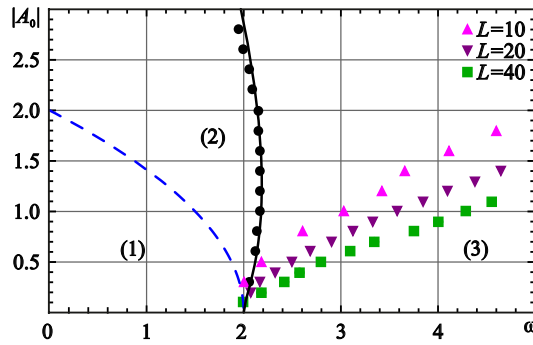


Fig 5. Domains of non-transmission (1), self-modulation (2), and steady-state transmission (3) on the $(\omega, |A_0|)$ parameter plane. The dashed line is the boundary of non-transmission (10). The solid line is the theoretical boundary of the change in the nature of MI. Triangles and squares correspond to numerical boundaries of the change in the nature of MI for the unmatched system at different lengths L , circles correspond to the matched system (color online)

the critical values ω_{cr} were calculated at different amplitudes $|P_0|$ and then using the relations (6) and (7), the corresponding dependence $\omega_{cr}(|A_0|)$ was found. However, it should be noted that the numerically found boundary of the change in the character of MI is quite different from the theoretical one. This is obviously explained by the fact that the theoretical analysis in the section 3 was carried out for boundless system, whereas the system with boundary conditions (4) and (5) is fundamentally bounded and has a finite length L . The reflection of the wave from the left boundary prevents the shift of perturbations along the system in the case of convective MI. Accordingly, the boundary of the establishment of stationary regime is significantly shifted to the region of higher frequencies, and the longer the length of the system, the more pronounced this effect is (see Fig. 5).

It is of interest to study the change in the nature of MI for a system that is matched on the left border, which allows to eliminate reflections. This can be achieved by smoothly changing the magnetic field along the system. Specifically, a matching section of length $Z_0 < L$ was added to the numerical model, on which the frequency detuning dependent on Z is introduced into the equation of motion:

$$\frac{\partial p}{\partial Z} + i(\Delta(Z) + |p|^2)p = a, \quad (19)$$

which was selected in the form of

$$\Delta(Z) = \begin{cases} \Delta_{\max}(Z_0 - Z)^2/Z_0^2, & 0 \leq Z \leq Z_0, \\ 0, & Z_0 \leq Z \leq L. \end{cases} \quad (20)$$

The dependence (20) simulates a smooth increase in the magnetic field in the region $0 \leq Z \leq Z_0$ along the direction of motion of electrons entering into the interaction space. At $Z = Z_0$, the magnetic field reaches a value corresponding to the cyclotron resonance, and then remains constant. In this case, the mismatch turns to zero.

Simulation of the matched system shows that with sufficiently long matching section, reflections are practically not observed. The numerical boundary of the change in the character of MI, shown in Fig. 5 by circles, agrees well with the theoretical one, and the simulation results practically do not depend on the parameters included in (20). The specifically presented results are obtained for $\Delta_{\max} = 2$, $Z_0 = 10$ and $L = 23$, that is, the length of uniform part of the system is 13.

Figure 6 illustrates the spatiotemporal dynamics of the field at different values of the input signal frequency for unmatched (*a, c, e*) and matched (*b, d, f*) system. For the matched system, only uniform section is shown, $Z_0 \leq Z \leq L$. The figures 6, *a, b* are plotted at $|A_0| = 1.0$ and $\omega = 1.5$, which corresponds to a point lying slightly above the transmission boundary in Fig. 5. In both cases, the development of MI leads to the generation of a periodic train of solitons. However, in the unmatched system, a partial reflection of the soliton from the left boundary and its propagation in the in the same direction in which the electron beam moves occurs that is clearly seen in Fig. 6, *a*. In the case of the matched system (see Fig. 6, *b*) it can be seen that solitons form near the right boundary, and then propagate along the system at a constant speed.

When increasing the frequency to $\omega = 2.5$ we get into the area of convective MI (see Fig. 5). However, in the unmatched system, due to the influence of the reflected wave, the stationary regime is not established. The formation of solitons does not occur, and fluctuations in the

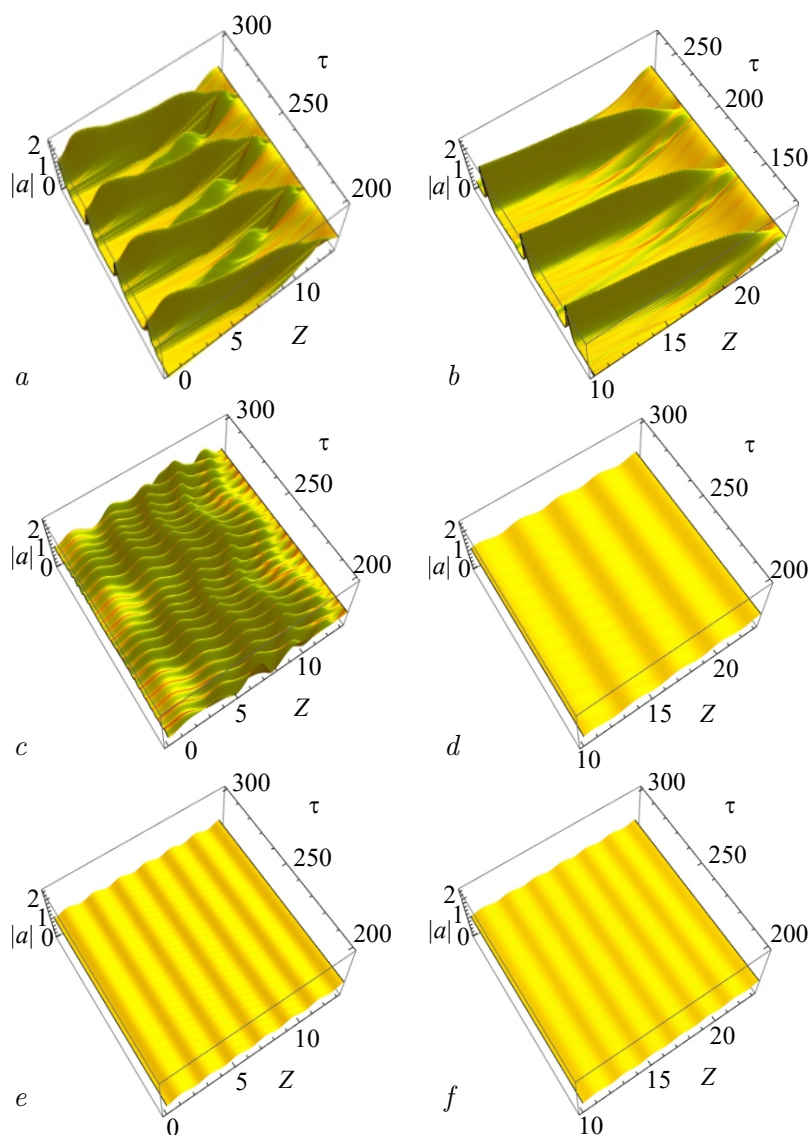


Fig 6. Spatiotemporal diagrams of the field amplitude at $|A_0| = 1.0$ and different values of the input signal frequencies: $\omega = 1.5$ (*a, b*), 2.5 (*c, d*), 3.5 (*e, f*). Figures (*a, c, e*) correspond to the unmatched system, (*b, d, f*) correspond to the matched system (color online)

amplitude of the field are complex, irregular in nature (see Fig. 6, *c*). The stationary regime is established in the matched system (see Fig. 6, *d*). At the same time, the amplitude periodically depends on the coordinate, which indicates the presence of a reflected signal, but its influence is small. The standing wave ratio (SWR), which is defined as the ratio of the maximum value of the amplitude to the minimum, is equal to 1.28.

At $\omega = 3.5$, the stationary regime is set for both matched and unmatched system (see Fig. 6, *e, f*). In both cases, the amplitude periodically depends on the coordinate, but for the matched system, this dependence is less pronounced: for the unmatched system, the SWR is 1.22, for the matched system, it is 1.13.

Conclusion

In this paper, MI is investigated in the interaction of an electromagnetic wave with a counterpropagating, initially rectilinear electron beam under the cyclotron resonance condition. The nonlinear nature of the dependence of the cyclotron frequency on the electron energy leads to a shift of the cyclotron absorption band and the manifestation of the effect of nonlinear tunneling with an increase in the power or frequency of the incident wave. A rigorous analysis of the nature of MI has been carried out. By analyzing the asymptotic form of perturbations calculated by the saddle-point analysis, the conditions under which MI is absolute or convective are found, and the boundary of the change in the character of MI on the plane of the input signal parameters is constructed.

Numerical simulation shows that with an increase in the frequency of the input signal, nonstationary self-modulation regimes that correspond to absolute MI are replaced by stationary single-frequency signal propagation due to convective MI. However, the fundamental influence of reflections in the spatially limited system complicates the comparison with theoretical conclusions. The simulation of the system matched at the boundary through which the electron beam enters is carried out. In this case, the boundary of the change in the character of MI is in good agreement with the theoretical dependence obtained from the analysis of the character of MI. In the matched system, the generation of periodic trains of solitons is facilitated. Such regimes are of interest from the point of view of generating frequency combs in the microwave range.

References

1. Benjamin TB. Instability of periodic wavetrains in nonlinear dispersive systems. Proc. R. Soc. Lond. A. 1967;299(1456):59–76. DOI: 10.1098/rspa.1967.0123.
2. Dodd RK, Eilbeck JC, Gibbon JD, Morris HS. Solitons and Nonlinear Wave Equations. London: Academic Press; 1982. 630 p.
3. Newell AC. Solitons in Mathematics and Physics. Philadelphia: SIAM; 1985. 260 p. DOI: 10.1137/1.9781611970227.
4. Ostrovsky LA, Potapov AI. Modulated Waves: Theory and Applications. Baltimore, MD, USA: The Johns Hopkins University Press; 1999. 369 p.
5. Zakharov VE, Ostrovsky LA. Modulation instability: The beginning. Physica D. 2009;238(5): 540–548. DOI: 10.1016/j.physd.2008.12.002.
6. Ryskin NM, Trubetskov DI. Nonlinear Waves. Moscow: URSS; 2021. 312 p. (in Russian).
7. Ryskin NM. Oscillations and Waves in Nonlinear Active Media. Saratov: Saratov University Publishing; 2017. 102 p. (in Russian).
8. Balyakin AA, Ryskin NM. A change in the character of modulation instability in the vicinity of a critical frequency. Tech. Phys. Lett. 2004;30(3):175–177. DOI: 10.1134/1.1707158.

9. Balyakin AA, Ryskin NM. Modulation instability in a nonlinear dispersive medium near cut-off frequency. *Nonlinear Phenomena in Complex Systems*. 2004;7(1):34–42.
10. Rostuntsova AA, Ryskin NM, Zotova IV, Ginzburg NS. Modulation instability of an electromagnetic wave interacting with a counterpropagating electron beam under condition of cyclotron resonance absorption. *Phys. Rev. E*. 2022;106(1):014214.
11. Newell AC. Nonlinear tunnelling. *J. Math. Phys.* 1978;19(5):1126–1133. DOI: 10.1063/1.523759.
12. Zotova IV, Ginzburg NS, Zheleznov IV, Sergeev AS. Modulation of high-intensity microwave radiation during its resonant interaction with counterflow of nonexcited cyclotron oscillators. *Tech. Phys. Lett.* 2014;40(6):495–498. DOI: 10.1134/S1063785014060285.
13. Zotova IV, Ginzburg NS, Sergeev AS, Kocharovskaya ER, Zaslavsky VY. Conversion of an electromagnetic wave into a periodic train of solitons under cyclotron resonance interaction with a backward beam of unexcited electron-oscillators. *Phys. Rev. Lett.* 2014;113(14):143901. DOI: 10.1103/PhysRevLett.113.143901.
14. Ginzburg NS, Zotova IV, Kocharovskaya ER, Sergeev AS, Zheleznov IV, Zaslavsky VY. Self-induced transparency solitons and dissipative solitons in microwave electronic systems. *Radiophysics and Quantum Electronics*. 2021;63(9–10):716–741. DOI: 10.1007/s11141-021-10092-w.
15. Benirschke DJ, Han N, Burghoff D. Frequency comb ptychography. *Nat. Commun.* 2021;12(1):4244. DOI: 10.1038/s41467-021-24471-4.
16. Hagmann MJ. Scanning frequency comb microscopy—A new method in scanning probe microscopy. *AIP Advances*. 2018;8(12):125203. DOI: 10.1063/1.5047440.
17. Gaponov AV, Petelin MI, Yulpatov VK. The induced radiation of excited classical oscillators and its use in high-frequency electronics. *Radiophysics and Quantum Electronics*. 1967;10(9–10):794–813. DOI: 10.1007/BF01031607.
18. KuzeleV MV, Rukhadze AA. *Methods of Wave Theory in Dispersive Media*. Singapore: World Scientific; 2009. 272 p. DOI: 10.1142/7231.
19. Barletta A, Celli M. Convective to absolute instability transition in a horizontal porous channel with open upper boundary. *Fluids*. 2017;2(2):33. DOI: 10.3390/fluids2020033.